

# Creep properties of fatigued short carbon fibre reinforced nylon 6 plastics

EIICHI JINEN

*Technical College, Kyoto Institute of Technology, Matsugasaki Sakyo-ku, Kyoto 606, Japan*

The effect of low-cycle fatigue on the creep properties of a fibre-reinforced thermoplastic has been examined from the standpoint of the stress dependence and cycle ratio, which is the fraction of the mean life cycles to fracture. The time dependence of the strain and the strain rate of a virgin specimen can be described by a straight line on a logarithmic scale, therefore the deformation process seems to be ruled by a flow law. In addition the time dependence of the strain rate does not indicate the stress dependence for each stress level, which shows the same value as in the gradient of these relations. In the case of fatigued specimens, however, a knee point which divides the creep process into a primary region and a secondary one appears in the creep relation. The gradient in the primary region is less than that for the virgin material, and the magnitude and the timing of its appearance show either a stress dependence or a cycle ratio dependence. A weak stress dependence of the relation for  $\log \epsilon$  against  $\log t$  can also be found; however, the results do not indicate a dependence on the cycle ratio. The reason for these results and the relationship of the structural changes of the materials are discussed using a McLean model.

## 1. Introduction

The mechanical behaviour of composites depends closely on microstructure such as the fibre aspect ratio, fibre content, fibre orientation and the fibre dispersal state in the matrix, and the adhesive or interface properties between the fibre and matrix. Many investigators have investigated the mechanics, physics and chemistry of the interface. For example, Kelly [1] derived a model for the debonding and pulling out of the fibres. This mechanism has attracted many researchers [2, 3], because the model is the most fundamental and the simplest one for estimating the reinforcing and toughening effect of the fibre. A discussion of the strength near the breakage point of a material, however, requires that the plastic deformation and the debonding process between the fibre and matrix must be checked because these phenomena will be considered critical to states in higher stress levels. Though the model is a useful concept for the consideration of the mechanism of reinforcement by short fibres, the problem of the strength or the mechanical behaviour of the material should be recognized from the viewpoint of the real state of the structure, that is, the situation of the dispersed fibres and the adhesive condition do not accord completely with the model.

In order to investigate the mechanical properties and to estimate the adhesive conditions, therefore, they must be checked by using real commercially available materials. In order to find, as a whole, the character of the interface effect or mechanical behaviour of the material, observations of the creep property should be made because through analysis of that process it is possible to clear up the deformation

characteristics of the material. Moreover, this characteristic nature depends closely on structural factors such as the fibre property, its size and the type of dispersion of the fibres and the difference of the toughness between the fibre and matrix [4]. On the other hand, the estimation of the material strength or the endurance for fatigue conditions also closely depend on these factors. The author has noticed an accumulated strain in the low-cycle fatigue of a fibre-reinforced thermoplastic (FRTP) which is introduced by cyclic deformation, and has examined these characteristics [5]. It was found that the deformation process is ruled by a rate relation which relates to the number of cycles, and its characteristics are similar to those in the creep process. It seems that the creep properties are due to the fatigue process; this makes clear the character of the interface effect in an FRTP and also shows the relation between the degree of damage and the change in these properties.

## 2. Experimental procedure

### 2.1. Material and specimen design

A tensile specimen is injection-moulded using nylon 6 pellets (3 mm) which contain 15 wt% carbon fibre (Toray CM 1001 T15) and its configuration is shown in Fig. 1. The moulding conditions are as follows: the temperature of the hopper is 210°C; the front, middle and nozzle parts of the cylinder are at 240, 230 and 250°C, respectively; the moulding pressure is 720 kgf cm<sup>-2</sup> (70.6 MPa); the cycle is 15 sec; the die temperature is 80 to 90°C, and the screw speed is 100 r.p.m. Moulded specimens are tested after pre-conditioning in a standard air-conditioned room for a year. As a result, the moisture content reaches an

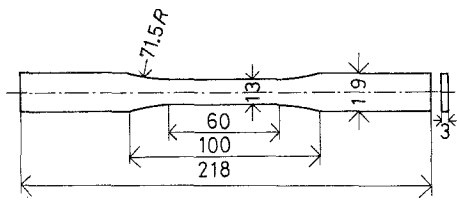


Figure 1 Specimen configuration. Dimensions in mm.  $R$  indicates the radius of curvature.

equilibrium content of about 3.5%. The tensile elastic modulus  $E$  is  $578 \text{ kgf mm}^{-2}$  (5.67 GPa), the tensile strength  $\sigma_B$  is  $9.1 \text{ kgf mm}^{-2}$  (89.2 MPa), the proof stress  $\sigma_{0.2}$  is  $5.1 \text{ kgf mm}^{-2}$  (50 MPa) and the elongation  $\phi$  is 7.5%.

## 2.2. Creep test

A creep test is conducted at the same stress as the stress amplitude in the previous fatigue test for the virgin specimen, and on specimens which were fatigued for a quarter, one-third and a half of the number of cycles of the average life ( $\bar{N}$ ), which is the stress and number relation of the fatigue test. The test specimen in creep is clamped at a distance of 130 mm, which is the same length as in the fatigue test, by two chucks. A 50 mm clip gauge is located in the gauge length and the measurement was performed by a moveable telescope. These instruments are arranged in a temperature-controlled box. The applied instruments are arranged in a temperature-controlled box. The applied tensile stresses on the specimen are 6.0, 6.5 and  $7.0 \text{ kgf mm}^{-2}$  (58.8, 63.7 and 68.6 MPa). A change in gauge length is detected by the relative motion between the ferromagnetic core and the coil part of a linear differential transformer. The output signal from the transformer is converted by a rectifying circuit and then fed into a d.c. recorder. Measurements are compared with calibrated values and the creep values are calculated after 1.5, 3, 6, 15, 21, 30, 42 sec and 1, 1.5, 2.5, 5, 10, 20, 40 min and 1, 2 h from the loading start. A creep rupture test is also conducted in the same way as the creep test; the lifetime and the creep of the specimen at failure are recorded.

## 2.3. Fatigue test

A Shimadzu Autograph IS-10T was used for tensile fatigue testing under load control. The test specimen is clamped by chucks and the gauge length is set at 50 mm. The periods of load deformation cycling for

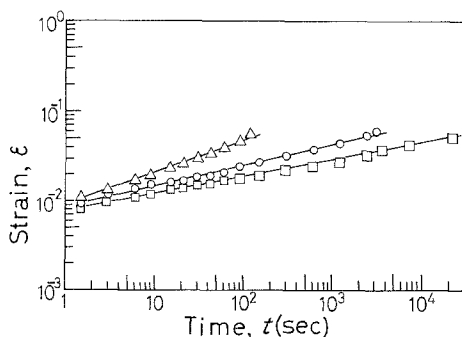


Figure 2 An example of creep relations for stress levels of  $\sigma =$  ( $\square$ ) 6.0, ( $\circ$ ) 6.5 and ( $\Delta$ )  $7.0 \text{ kgf mm}^{-2}$  in virgin specimens.

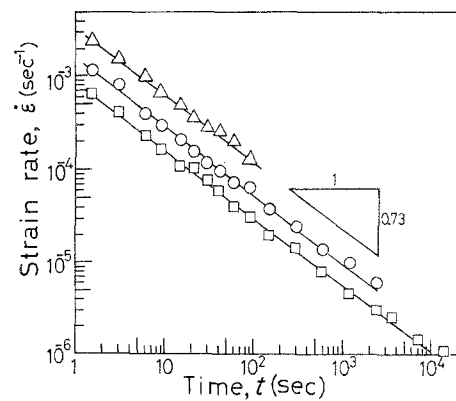


Figure 3 The strain rate-time relations for stress levels of  $\sigma =$  ( $\square$ ) 6.0, ( $\circ$ ) 6.5 and ( $\Delta$ )  $7.0 \text{ kgf mm}^{-2}$  in virgin specimens.

the stress levels 6.0, 6.5 and  $7.0 \text{ kgf mm}^{-2}$  are 4.5, 5.6 and 6.7 sec per cycle, respectively. Thus, the magnitude of the strain rate using these repeated cycles corresponds to about 0.56, 0.58 and  $0.62\% \text{ sec}^{-1}$ , respectively. The temperature change of the specimen surface during fatigue is measured at frequent intervals with a thermistor thermometer which has a small flat pick up mechanism. Both creep and fatigue tests were conducted at  $20 \pm 1^\circ \text{C}$ ,  $60 \pm 5\%$  relative humidity.

## 3. Experimental results

### 3.1. $S-N$ relation in low-cycle fatigue

The number of cycles to fracture is observed. The stress  $S$  and the number of cycles to fracture  $N$  in the so called  $S-N$  relation is shown in Fig. 2 [5]. Thus, the average number of cycles to fracture for stress levels of 6.0, 6.5 and  $7.0 \text{ kgf mm}^{-2}$  with ten specimens each is 34 800, 9744 and 760, respectively. Furthermore, the stress dependence of these average numbers of cycles indicates an almost negative linear relation on a semi-logarithmic scale.

### 3.2. Creep properties of the virgin specimen

#### 3.2.1. Strain-time relation

An example for stress levels of 6.0, 6.5 and  $7.0 \text{ kgf mm}^{-2}$ , plotted on a log-log scale, is shown in Fig. 2. These relations indicate the characteristic nature of the material, i.e. the deformation process is ruled by a logarithmic uni-process, which from the start of loading to the point of failure shows that the gradient of the linear relation increases with an increase in the stress level. Moreover, the strain at failure of specimens indicates almost the same value as is seen in each relation (6 to 7%). This result seems to confirm the relationship between structural factors for the material and the deformation process.

#### 3.2.2. Strain rate-time relation

The strain rate of every observation time is obtained by reading graphically the magnitude of the gradient in the second line of the creep curve, which is described on a normal scale. The results for stress levels of 6.0, 6.5 and  $7.0 \text{ kgf mm}^{-2}$  are shown in Fig. 3. Each plot indicates the average value for ten specimens. Fig. 3 denotes some of the significant characteristics of the creep property of the material, and the following

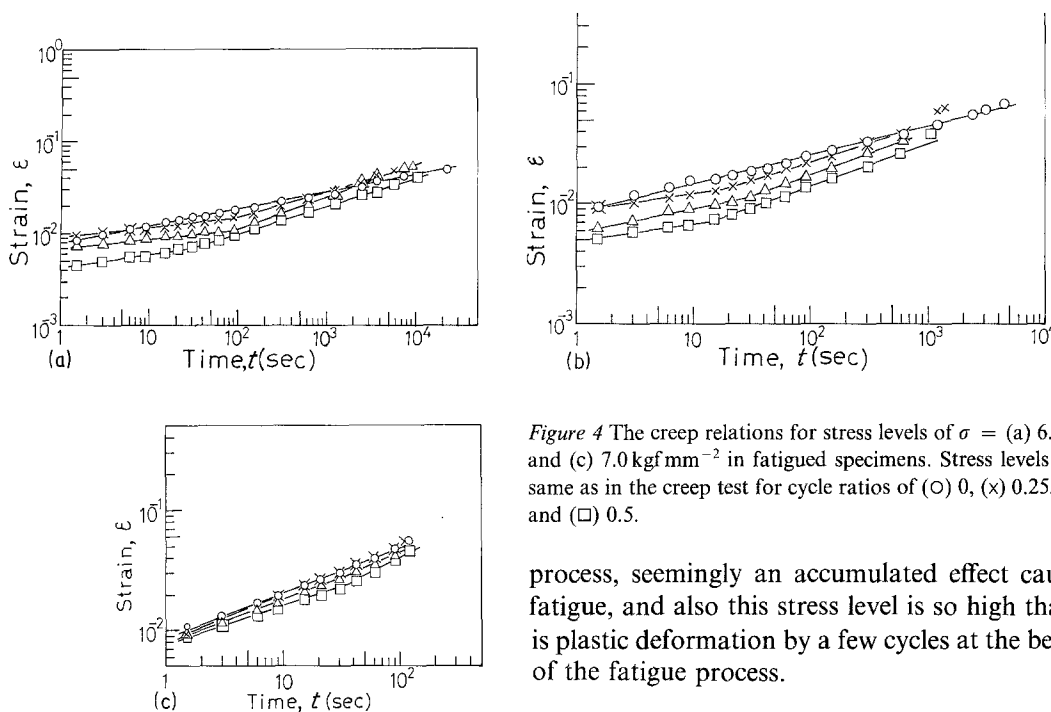


Figure 4 The creep relations for stress levels of  $\sigma =$  (a) 6.0, (b) 6.5 and (c) 7.0 kgf mm<sup>-2</sup> in fatigued specimens. Stress levels were the same as in the creep test for cycle ratios of (O) 0, (x) 0.25, ( $\Delta$ ) 0.33 and ( $\square$ ) 0.5.

points are observed: (a) the time dependence of the strain rate shows a negative linear relation on a log-log scale; (b) the magnitude of the gradient of the plotted line indicates almost the same value ( $-0.73$ ), so the time dependence of the relation is indicated by the stress level; and (c) moreover, the location of these plotted lines depends on the stress level and this position shifts to the upper side of the strain rate scale with an increase in the stress level. These results imply that the creep property of the material seems to be ruled by a uni-process or in other words a rate process, so it is possible to superpose all of the plots on an arbitrary line by shifting the time or the strain-rate scale.

### 3.3. Creep properties of the fatigued specimen

#### 3.3.1. Strain-time relation

The results for the virgin specimen and for fatigued specimens which are damaged for cycle ratios of a quarter, one-third and a half under the given stress levels of  $\sigma = 6.0, 6.5$  and  $7.0$  kgf mm<sup>-2</sup> are shown in Figs 4a, b and c, respectively. In general, the strain-time relation for the fatigued specimen occupies a lower position than for the virgin one, and the position depends on the degree of the fatigue damage. Also, a tendency of the plots to shift to the lower strain side with an increase in the fatigue damage can be found. This tendency is revealed more strongly in the beginning period of the creep process at the lower stress level, and a knee point can be found in the results for stress levels of  $6.0$  and  $6.5$  kgf mm<sup>-2</sup>. The location of this feature shifts to the lower side of the cycle with an increase in the degree of the fatigue damage or the stress level. This result denotes a different character in the creep process from that of the virgin specimen. However, at the stress level of  $7.0$  kgf mm<sup>-2</sup> such a tendency disappears from the plots. The reason for this tendency seems to be related to a phenomenon which occurs in the early region of the deformation

process, seemingly an accumulated effect caused by fatigue, and also this stress level is so high that there is plastic deformation by a few cycles at the beginning of the fatigue process.

#### 3.3.2. Strain rate-time relation

The plots using an average value of ten specimens for stress levels of  $\sigma = 6.0, 6.5$  and  $7.0$  kgf mm<sup>-2</sup> are shown in Figs 5a, b and c, respectively. In these figures, the change of the relation due to the different degree of damage by fatigue for cycle ratios of a quarter, one-third and a half are also indicated in each figure.

The following conclusions follow: (a) the creep process for the fatigued specimen can be described by a linear relation on a log-log scale, and (b) the stress dependence of the relation shows the same tendency as is seen in the results for the virgin specimen; that is, the plotting array shifts to the large strain rate side with an increase in the stress level. This result is similar to the one in Fig. 3. However, we observed a most interesting tendency. If one notices the magnitude of the gradient of these lines and compares it with the results for the virgin specimen, one can find a change in the size of the magnitude in Fig. 5 which is usually less than those in Fig. 3c. That is, the gradient of the plot seems to be related to the stress level or to the degree of damage of the material in the fatigue process. In general, the gradient decreases with an increase in the fatigue damage.

These results can be summarized in terms of the stress dependence of the magnitude of the gradient of the line ( $\log \dot{\epsilon}$  against  $\log t$ ), as shown in Fig. 6. This figure shows a significant effect for the characteristic change of the creep property due to fatigue damage. That is, the stress dependence of the virgin specimen is hardly discernible under the given stress conditions; however, for the fatigued specimens a weak negative linear dependence is indicated. Moreover, no change in the slope of the line for the three different degrees of fatigue damage seems to occur, but it only shifts to the lower value side of the gradient axis while a continuation of the fatigue process occurs. The shift value of these lines shows a large change in the low-cycle ratio of the fatigue damage, and this tendency denotes a saturation phenomenon because it can be found that

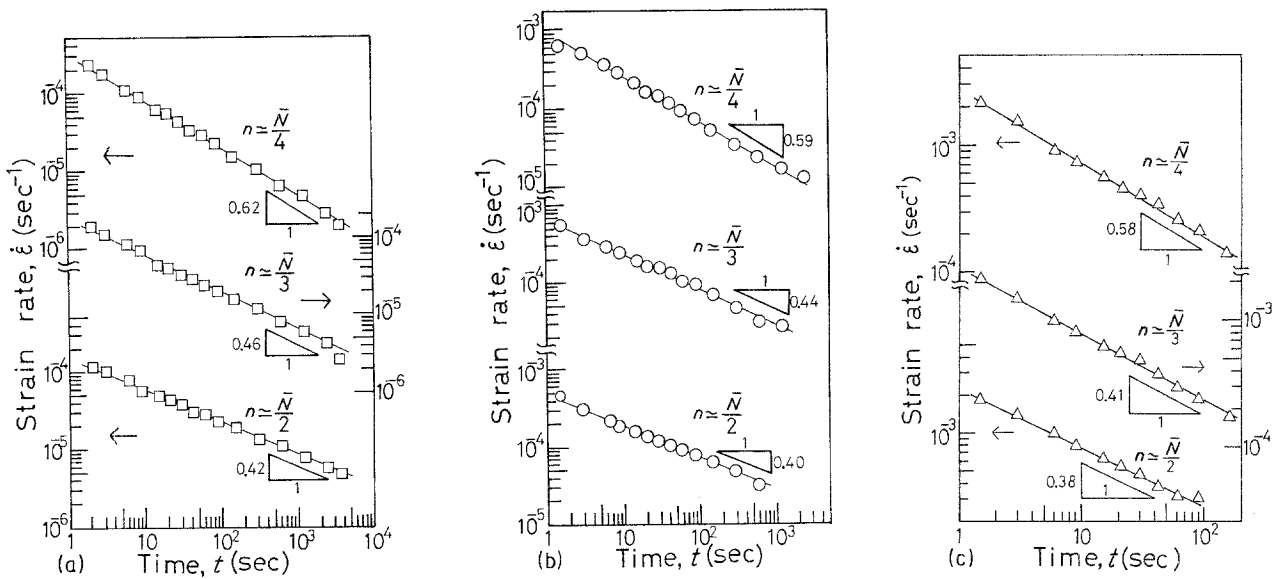


Figure 5 The strain rate–time relations for stress levels of  $\sigma =$  (a) 6.0, (b) 6.5 and (c) 7.0  $\text{kgf mm}^{-2}$  in fatigued specimens. Stress levels were the same as in the creep test for cycle ratios of 0.25, 0.33 and 0.5.

the interval of the location between the lines for a half and one-third of the cycle ratio is narrower than for the zero and the quarter values. These results will be discussed in a later section from the viewpoint of the relationship between the character change in the creep property and the structural change in the material due to fatigue damage.

### 3.4. The stress dependence of the rupture time

As is well known, the rupture time in the creep process is defined as a time interval in which a material is able to withstand a prolonged load, so it is an endurance test under a constant load or stress field on the material. Moreover, this factor is also relevant as a parameter which indicates the reliability, and the scatter of the plots is also useful as a parameter which denotes the homogeneity of the material. The stress dependence of this factor for the virgin specimen and fatigued ones with three different degrees of damage, plotted on a semi-log scale, is shown in Fig. 7. The plotting symbols in the figure denote the scattering of the time at each given stress level; each line shows the average value for about 10 specimens. These results show a linear stress dependence and an interesting observation can be made as follows: the gradients of

these lines seem to show almost the same value, and the location of the plot shifts to the short-life side with an increase in the fatigue damage.

## 4. Discussion

In order to discuss the changes of the creep properties due to fatigue damage, the characteristic features of the structural factors or the components of the material and the contribution of these factors to the mechanical properties should be recognized. The specimen is moulded into a slender shape by an injection process and a short carbon fibre is used as the reinforced material. Although all the dispersed fibres do not orient exactly parallel with each other, the direction seems to be parallel to the general longitudinal axis of the specimen. The direction of many fibres therefore seems to be mainly in the flow direction of the melted material during the die process, and it also corresponds to the direction of the tensile load. In FRTP, the reinforcement effect for material deformation under a stress field appears to be caused by the restriction by many dispersed fibres of the matrix viscous flow in the interface, or to intermittence between the fibre and matrix or fibre and fibre. Let us now recall McLean's model [6] and his treatment of

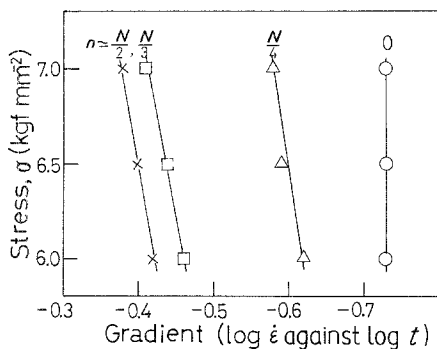


Figure 6 The stress dependence of the slope in the relation for  $\log \dot{\epsilon}$  against  $\log t$  in fatigued specimens. Stress levels were the same as in the creep test for cycle ratios of (O) 0, ( $\Delta$ ) 0.25, ( $\square$ ) 0.33 and ( $\times$ ) 0.5.

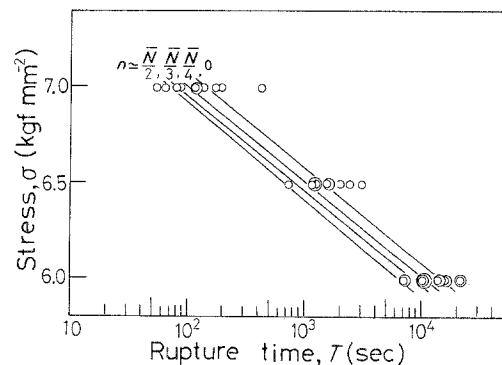


Figure 7 The stress dependence of rupture time in fatigued specimens. Stress levels were the same as in the creep test for cycle ratios of 0, 0.25, 0.33 and 0.5. Rows of small circles indicate the distribution of the results for the virgin specimen at each stress level.

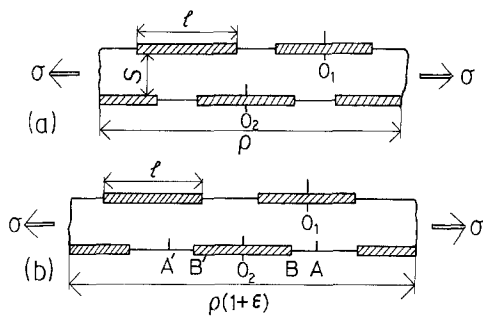


Figure 8 A schematic representation of a McLean's model [6]. An element of fibre-strengthened composite loaded in a tensile condition (a) before extension and (b) after extension  $\epsilon$ .

the problem of viscous flow and the interaction between the fibre and matrix.

His model considered the element of a fibre-strengthened solid, a segment of which is shown in Fig. 8a, which under tensile loading increased in length from  $\rho$  in Fig. 8a to  $\rho(1 + \epsilon)$  in Fig. 8b. The fibres themselves are supposed to be rigid, and for the moment the matrix is supposed to extend uniformly. This makes the assumption that the consequent relative motion between the matrix and fibre is symmetrical about the centre point of the fibre. The correctness of this assumption depends on the neighbouring fibres being distributed uniformly. At the centre of a fibre, e.g.  $O_1$  or  $O_2$ , there is then zero relative motion, but at the fibre end, a point in the matrix such as A in Fig. 8 moves away from the end to A' and there is relative motion A'B' between the fibre and the matrix. At any point initially at distance  $X$  from the fibre centre, there is relative motion

$$r = \epsilon X \quad (1)$$

The mean value of  $r$  is

$$\bar{r} = \epsilon l/4 \quad (2)$$

where  $l$  is the fibre length. Since the fibres are rigid, any point in a fibre will serve as a reference point from which to measure its relative motion, but the matrix does not extend uniformly as is supposed in Fig. 8b unless at the interface between the matrix and the fibre there is a completely uninhibited sliding. In so far as two adjacent fibres such as the two depicted in the figure can be considered, the centre line between the fibres is symmetrically disposed with respect to both fibres and therefore contains reference points in the overlapping region, which are suitable because they give the same answer for either fibre. The relative motion  $r$  in Equation 1, then involves a shear strain in the matrix of magnitude  $\gamma_c = 2r/S$ , where  $S$  is the spacing between the fibres. Substitution in Equation 2 gives the average matrix shear strain  $\gamma_c$  in the fibre-strengthened material as

$$\gamma_c = \epsilon l/2S \quad (3)$$

In a separate block of the matrix the shear strain accompanying an extension is  $\gamma_c = 2\epsilon$ . Comparison with Equation 3 shows that in the fibre-strengthened material the shear strain is magnified by the factor

$$\gamma_c/\gamma_0 = l/2S \quad (4)$$

Consideration of the reinforcement effect in a model fibre-strengthened material is discussed for a static condition; however, this shear magnification must also clearly apply to the shear strain rates. That is, from this the amplification of the shear strain rate and the amplification of the shear stress can be obtained by using a flow law, which often approximates a power law connecting the shear stress  $\tau$  with the strain rate  $\dot{\gamma}$ :

$$\dot{\gamma} = \alpha \tau^n \quad (5)$$

where  $\alpha$  and  $n$  are experimentally determined constants. Therefore

$$\tau_c = \left(\frac{\dot{\gamma}_c}{\alpha}\right)^{1/n} = \left(\frac{l\dot{\gamma}_0}{2S}\right)^{1/n} = \left(\frac{l}{2S}\right)^{1/n} \tau_0 \quad (6)$$

using Equations 4 and 5 and applying the ratio in Equation 4 to the strain rates. The shear stress in the composite is consequently magnified by the factor

$$\frac{\tau_c}{\tau_0} = \left(\frac{l}{2S}\right)^{1/n} \quad (7)$$

On the other hand, the discussion of the stress system in the fibre-strengthened matrix is performed by calculating in terms of the energy dissipated during the flow. Then, stress  $\sigma_c$  applied to an unsupported matrix increases according to the speed  $\dot{\epsilon}$ , and the rate at which work is done is  $\sigma_0 \dot{\epsilon}$  per unit volume. Similarly for the fibre-strengthened matrix the rate of work is  $\sigma_c \dot{\epsilon}$  per unit volume,  $\sigma_c$  being the tensile stress required to produce the extension at a rate of  $\dot{\epsilon}$ . Let  $\tau_0$  and  $\dot{\gamma}_0$  be the shear stress and shear strain rates in the unsupported matrix at  $45^\circ$  to the tensile axis;  $\tau_0 = \frac{1}{2}\sigma_0$  and  $\dot{\gamma}_0 = 2\dot{\epsilon}$ . We therefore have

$$\sigma_0 \dot{\epsilon} = \tau_0 \dot{\gamma}_0 \quad (8)$$

Here, let  $\tau_c$  and  $\dot{\gamma}_c$  be the significant shear stress and strain rates in the fibre-strengthened matrix, respectively. They must then be produced by the term  $V_m$ , the matrix volume fraction, introduced because the energy is assumed to be expended only in the matrix. Therefore, inserting in Equation 8 the amplification factors for the strain and stress, that is, substituting  $\tau_c$  from Equation 7 and  $\dot{\gamma}_c$  from Equation 4 we have

$$\frac{\sigma_c}{\sigma_0} = V_m \left(\frac{l}{2S}\right)^{1+(1/n)} \quad (9)$$

Here, consider the changes of the relation between the mechanical condition and the structural one due to the fatigue damage of the material. As shown in Figs 2 and 3, the time dependence of the strain rate for the virgin specimen can be described by a linear relation on a log-log scale. So, the deformation process seems to be ruled by a flow law which is expressed approximately by Equation 5. However, the results for the stress levels of 6.5 and 6.0 kgf mm<sup>-2</sup> in the fatigued specimen show a knee point in the time dependence of the strain; also, in the prior region before the knee point, the magnitude of the gradient in the relation is usually less than that for the virgin specimen. This tendency seems to increase with the stiffness of the material, and the phenomenon seems to be related to the fatigue effect or to an accumulated effect due to repeated deformation with the many

cycles performed before the creep. The phenomenon of an increase in the stiffness caused by the fatigue effect in this material, as shown in a previous report [5], can also be easily found in the change caused by a rise in the portion of the stress-strain relation by means of a monotonously increasing load system. So, the reason for the increase in the stiffness of the material should be discussed now.

It is necessary to point out that the fatigue effect in damaged FRTP appears at the interface between the fibre and matrix in the first stage. Therefore the experimental results have been treated from the points of view of the following model treatments. The results of Figs 2 and 3 indicate that the fatigued specimen shows a larger value than the virgin one for the same loading time. This result implies that the increase in the stiffness of the material is caused by fatigue and also increases the magnification factor for the shear stress in Equation 7.

In order to clear up the reason for this and to consider the relationship between structural factors and the results, it must be pointed out that a decrease in the  $S$  value (the spacing between fibres) or a change in fibre length must be examined. In the case of a low-cycle fatigue under a stress amplitude that is higher than is usually used, the total strain value is composed of the component due to elastic deformation and also that due to plastic deformation. The plastic deformation increases and adds an accumulated strain in every cycle as a certain amount of strain remains. On the other hand, in the vertical direction of loading a shrinkage phenomenon which depends on the Poisson's ratio of the material occurs and the contraction will increase. Such so-called fatigue effects may remain in the beginning stage of the creep. Moreover, in the case of this specimen, many short carbon fibres orient mainly in the loading direction, so the contraction phenomenon seems to introduce a decrease in the space between the fibres. On the other hand, the effect of the decrease of fibre length due to the progress of the fatigue process on the amplification factor for the shear strain ratio in the fibre-strengthened material contributes to a reverse tendency in the change of the  $S$  value.

Though the fibre structure of the material differs from our specimen, the model also applies to the problem of the change of fibre strength (not fibre length) in the fatigue process of a material which is reinforced by a hybrid structure with a carbon fibre/glass fibre; see the paper by Hiwa *et al.* [7], which reported the relation between the fibre strength and the cycle ratio ( $n/N$ ). The changes of the fibre strength show an inverse proportional relation. The decreases of the fibre strength in the hybrid or glass fibre reinforced (GFRP) structures are from 1000 to 1100 MPa down to 600 to 700 MPa, and these values correspond to an increase of the cycle ratio from 0 to 0.2, respectively. That is, a large decrease in the fibre strength appears in an early stage of the cycle ratio; in the latter stages, that is for those with a cycle ratio of over 0.4, the decreasing tendency became a moderate one and approaches a constant value. As the change of the fibre strength has a close relation to the fibre length, so also it seems that a similar relation exists

between the changes in the fibre length and cycle ratio. In these experiments we deal with specimens which have been fatigued from a quarter to a half of the mean life cycle. Therefore, the changes of the fibre length in this stage may be smaller than those in an earlier stage. If these findings are accepted, the reason for the increase of the stiffness by repeated deformation in a low-cycle fatigue may be interpreted from the experimental results in Figs 2 and 3 by a decrease in the fibre spacing, i.e. of the  $S$  value as mentioned above.

The next discussion is a consideration of the reason for the appearance of the knee point which can be seen in Figs 4a and b. When the fatigue tests have been interrupted, an accumulated strain which arose in that process will be diminished by the disappearance of the elastic strain and some shrinkage which occurs with a relaxation phenomenon. Such a situation may hold in the specimen as a fatigue effect before the creep. When the creep deformation reaches a value which corresponds to the previous remaining deformation due to the fatigue process, the creep process will enter into a new stage, because at this stage the size of the deformation may be enlarged due to fatigue damage. The strain value in this stage seems to be about 7 to 8%. It is considered that the deformation process in the new stage does not correspond to a local or limited viscous flow of the matrix between the aligned fibres, but to a large portion of an area in the fibre-strengthened material which is enclosed by a few fibres and to the beginning of cracking which extends perpendicular to the loading direction.

The model shown in Fig. 8 may not therefore be used in the interpretation of the deformation mechanism of the material. Therefore, the magnitude of the gradient in the creep relation will become larger than that in the previous stage. In fact, as is shown in Figs 4a and b, the gradient of the line for the second stage of the fatigued specimen indicates a larger slope than that for the first stage, and also that for the virgin specimen. As mentioned above, it is understood that the reason for the appearance of the knee point in the creep relation indicates a change of the deformation mechanism in the creep process, due to the pre-damage of the material which it underwent in the previous stage before the creep. The timing of the appearance of this knee point depends on the cycle ratio; as shown in Fig. 4, the higher the cycle ratio of the fatigue damage, the earlier is the stage of the creep process that will appear.

In the results for the stress level of  $7.0 \text{ kgf mm}^{-2}$ , as shown in Fig. 4c, a characteristic knee point cannot be found. In order to establish the reason for this, the value of the creep strain at the knee point should be noted. That is, in the case of this stress level, the strain amounts are about 8 to 9% even in the beginning or transient stages of the creep process. This value is surpassed by that at the appearance of the knee point, which can be seen in the result for the stress levels of  $6.5$  or  $6.0 \text{ kgf mm}^{-2}$ . Therefore, this result shows that the stress level of  $7.0 \text{ kgf mm}^{-2}$  is a very high-stress condition for the material.

Another interesting result for the time dependence of the strain rate should be noted. As shown in Figs 3

and 5, the characteristic feature of the relation indicates that the process can be described as a uni-process by a straight line on a log scale for both cases, the virgin specimen and the fatigued one. This result implies that the character of the creep process is ruled basically by a flow law which is expressed by Equation 5. In the case of the virgin specimen, it is understood from the result in Fig. 3 that the magnitude of the gradient in such straight lines (i.e. the  $n$  value) does not show a stress dependence. On the other hand, as a general tendency, the  $n$  value for the fatigued specimen shows a weak negative dependency and the tendency increases with an increase in the stress level. Another interesting result is that this stress dependence is independent of the cycle ratio, and the relations at each stress level are parallel with each other on the normal scale as shown in Fig. 6. Also, the straight line shifts to the lower value side of the magnitude of the gradient with an increase in the cycle ratio of the fatigue process.

The shift of the value of these straight lines due to the progress of the fatigue process shows a saturation phenomenon, that is the distance between the line for the virgin specimen and the one for the cycle ratio is a quarter wider than the one between the two lines for the one-third and the one-half cycle ratios. This fact seems to indicate that there is an influence of an increase in the stiffness of the material. Moreover, the relation in Equation 8 indicates the energy balance of the continuation of the deformation process of the material with the working value by loading products aligned with the movement of the crosshead of the machine. The consumption of this energy occurs in the matrix, therefore the parallel location of these straight lines (shown in Fig. 6) can be interpreted in terms of the volume fraction of the matrix, because the value for the specimen is the same as under one condition only. As mentioned above, the repeated deformation of the dispersed reinforced material due to the fatigue process accumulates a viscous flow of the matrix within the fibre-strengthened material. On the other hand, this phenomenon introduces a decrease in the fibre spacing, so the stiffness which works against the deformation of the material seems to increase. It is also found that a McLean model is a useful tool for the interpretation of these experimental results. Furthermore, the differences of the fracture surface in the fatigue process and the ruptured one following creep of the specimen have been examined in regards to the hole size or its configuration due to the pulling out of the fibres by observation with a scanning electron microscope [5].

## 5. Conclusions

In order to clear up the cause of the fatigue mechanism of an FRTP, the creep properties of a low-cycle fatigued short carbon fibre reinforced nylon 6 are examined at room temperature in regard to the changes of the time dependence of the strain or the strain rate, from the standpoints of the stress level and cycle ratio which is used as a parameter to ascertain the degree of damage to the material. McLean's model [6] is applied in the interpretation of the experimental data, and

below the results which were obtained are given together with some discussion to explain them.

For material in its virgin state, the creep process and the time dependence of the strain rate are uni-processes and can be described with a straight line on a log plot, so the character of the creep relation is basically ruled out by a flow law. The creep relation obviously shows a stress dependence; however, the strain rate-time relation which can be obtained by a graphical method from a creep curve on a normal scale is not followed, and three lines for stress levels  $6.0 \text{ kgfmm}^{-2}$  (58.8 MPa), 6.5 (63.7) and 7.0 (68.6) occupy parallel locations. The position shifts to the lower value side of the strain rate axis with a decrease in the stress level.

In the case of the fatigued specimen, however, the creep relation cannot be described by a straight line on a logarithmic scale but a knee point can be seen except at higher stress levels. The reason for the appearance of the knee point implies the existence of a difference in the creep process. That is, in the primary region before the appearance of the knee point, the magnitude of the gradient of the line for the creep relation is usually less than that for the virgin specimen. In addition, the magnitude of the gradient of the straight line for the primary region depends on the cycle ratio; the size of the gradient decreases with the cycle ratio. On the other hand, in the second region after the knee point, this tendency became an inverse one. It is thus found that the fatigue effect due to repeated cycles produces an increase in the stiffness of the material. Moreover, this effect can also be seen in the strain rate-time relation which has a weak negative stress dependence. That is, the magnitude of the gradient of the straight line indicates the same values, though the location of these lines for each cycle ratio shifts rapidly to the lower value side with an increase in cycle ratio. In order to interpret these experimental results an increase of stiffness in the fatigue process and the relationship between the structural changes of the material and a McLean model have been discussed.

## Acknowledgements

The author wishes to thank Junichi Matsui and Sadao Arai of the Toray Co. Ltd for supplying and arranging for the injection of the specimens. Thanks are also due to Professor Meguma Suzuki of the Kyoto Institute of Technology for his encouragement. This work was supported in part by a Grant-in-Aid for Science and Research from the Ministry of Education, Japan.

## References

1. A. KELLY, *Proc. R. Soc.* **A310** (1970) 95.
2. P. LAWRENCE, *J. Mater. Sci.* **7** (1972) 1.
3. J. K. WELLS and P. W. R. BEAUMONT, *ibid.* **17** (1982) 397.
4. A. TAKAKU and R. G. C. ARRIDGE, *J. Phys. D., Appl. Phys.* **6** (1973) 2038.
5. E. JINEN, *J. Mater. Sci.* **21** (1986) 435.
6. D. McLEAN, *ibid.* **7** (1972) 98.
7. C. HIWA, K. ASAKA and T. NAKAGAWA, *J. Soc. Mater. Sci. Jpn* **34** (1985) 59.

Received 17 June  
and accepted 11 November 1986